LAUTECH Journal of Engineering and Technology 20 (1) 2026: 219 - 234

10.36108/laujet/6202.02.0191

Adsorption of Phosphorus from Palm Oil Mill Effluent Using a Blended Bio-Inorganic Adsorbent

[1*]Akande O. G., [1]Eletta O. A. A., [1]Tijani I. A., [1,2]Babatunde E. O. and [1]Adewoye T. L.

[1]Department of Chemical Engineering, Faculty of Engineering and Technology, University of Ilorin, Ilorin, Nigeria

[2]Department of Chemical Engineering Technology, Doornfontein Campus, Faculty of Engineering and Built Environment, University of Johannesburg, 2028 South Africa

Article Info

Article history:

Received: Dec 31, 2025
Revised: Jan 30, 2026
Accepted: Apr 30, 2026

Keywords:

Palm Oil Mill Effluent, Adsorption, Bio-Inorganic Blended Adsorbent, Phosphorus, Kinetics And Isotherm

Corresponding Author:
ogakande001@gmail.com

ABSTRACT

The discharge of palm oil mill effluent (POME), which is rich in phosphorus, into water bodies contributes to eutrophication and harmful algal blooms. This study investigates the characterization and adsorption performance of a low-cost kaolinite-banana peel biochar as a blended bio-inorganic adsorbent for phosphorus removal from POME. The blended adsorbent was characterized using Fourier Transform Infrared Spectroscopy (FTIR), Scanning Electron Microscopy (SEM) and Energy Dispersive Spectroscopy (EDS). Batch adsorption experiment was conducted to evaluate the effects of contact time (60-135 min), adsorbent ratio (KC:BP of 1 g total) and agitation speed (100-200 rpm). The optimum conditions were identified as 90 min contact time, 0.75:0.25 g (KC:BP) ratio and 175 rpm agitation speed achieving 88% phosphorus removal and reducing concentration from 51.72 mg/L to 6.12 mg/L. The corresponding adsorption capacity was calculated as 2.38 mg/g. Adsorption kinetics were best described by the pseudo second order model indicating that chemisorption may play a dominant role. Isotherm analysis showed that the Temkin model provided the best fit suggesting adsorbate-adsorbent interactions with decreasing heat of adsorption. Reusability studies revealed a gradual decline in adsorption efficiency with significant performance loss observed after the second cycle. The results demonstrated that the blended kaolinite clay and banana peel biochar has strong potential as a low-cost and sustainable adsorbent for phosphorus removal from complex wastewater systems like POME.

INTRODUCTION

The oil palm industry is one of the major agricultural sectors in several regions of the world including Malaysia, Indonesia, Thailand, Colombia and Nigeria (Utibe *et al.,* 2024). Proximity to source of water is regarded as one of the key factors that determines the location of the oil palm industry. The production of oil palm has led to rapid development and economic growth in producing nations (Utibe *et al.,* 2024). While the oil palm industry remains highly profitable, its significant environmental impact cannot be ignored. Oil palm processing generates three primary waste streams: solid waste (empty fruit bunches, palm press fibers, chaff, and palm kernel shells), liquid waste (palm oil mill effluent), and gaseous emissions from mechanized operations, agrochemical use and processing activities (Okereke & Ginikanwa, 2020).

Palm Oil Mill Effluent (POME) has been identified as a major contributor to water pollution due to the discharge of untreated effluent into rivers (Norhafezah *et al.,* 2023). It is a thick, brown liquid, usually discharged at 80–90 °C with a pH of 4.0–5.0, rich in nutrients (potassium, phosphorus, and nitrogen), as well as biological oxygen demand, chemical oxygen demand and oil and grease (Mohammad *et al.,* 2021). POME is obtained during

the clarification stage of oil palm extraction, where the fluid that comes out from the pulp pressing is a mixture of oil palm, water, cell debris, fibrous material and non-oily solids (Biodiin *et al.,* 2021). In Western Nigeria, most of the POME generated by small-scale traditional operators is discharged directly into the surrounding environment without treatment. High nutrient concentrations in water bodies can contribute to eutrophication, leading to algal overgrowth and oxygen depletion (Singh *et al.,* 2021).

Phosphorus is one of the essential nutrients for life, as it supports many cellular processes. However, its excessive release into the environment poses a serious environmental challenge (Zahed *et al.,* 2022). Excess phosphorus accelerates eutrophication, stimulating algal blooms which deplete dissolved oxygen and disrupt aquatic ecosystems (Singh *et al.,* 2021). This has become a critical parameter in the assessment and treatment of POME, underscoring the need for effective removal or recovery strategies (Abdoli *et al.,* 2021). Most researches on POME management has focused on reducing organic load, oil and grease, and other pollutants using conventional methods (Kasmuri *et al.,* 2023; Edet *et al.,* 2020; Norhafezah *et al.,* 2023). Comparatively, fewer studies have addressed phosphorus as a targeted pollutant of concern. Existing treatment methods often fail to achieve satisfactory nutrient removal, leaving residual phosphorus that continues to drive eutrophication risks. This gap underscores the need to explore efficient and sustainable methods for phosphorus adsorption and recovery.

Adsorption is considered an effective wastewater treatment method due to its universal applicability, cost-effectiveness, ease of operation, ability to remove both soluble and insoluble organic pollutants with efficiencies up to 99.9%, and simple design and operational convenience (Ali *et al.,* 2019). Several studies have explored the use of kaolinite clay and banana peel biochar individually for pollutant removal (Al-Swadi *et al.,* 2023; Kataya *et al.,* 2023; Song *et al.,* 2020; Ogundipe *et al.,* 2023; Narayana, 2022; Selvarajoo *et al.,* 2019). These studies showed that these materials exhibit high microporosity, stability, a large surface area, high cation-exchange capacity, and a rich array of functional groups. However, limited attention has been given to their combined application for phosphorus removal from untreated POME.

Futhermore, the adsorption mechanism, rate-controlling steps and equilibrium behavior were not fully explored. The adsorption kinetics and isotherm are important to provide insight into the interaction between the adsorbate concentration and the adsorbent's capacity at a fixed temperature and to understand the rate at which a solute is removed from solution which is usually influenced by the contact time between the adsorbate and the solid adsorbent (Saleh, 2022; Al-Ghouti *et al.,* 2020; Eletta *et al.,* 2016). Therefore, this study aims to investigate the adsorption of phosphorus from palm oil mill effluent using a blended bio-inorganic adsorbent.

MATERIALS AND METHODS

Wastewater characterization

The palm oil mill effluent was collected from an oil palm mill in Oke-Ila Orangun, Ifedayo Local Government Area, Osun State. The characterization of the wastewater was conducted at the Integrated Research Laboratories in Ilorin, Nigeria. Solvent (distilled water) and Reagent (ammonium molybdate and potassium antimony) were used to determine the phosphorus content in the POME to know if the targeted pollutant is higher or lower than the permissible limit of the National Environment Standard Regulations Enforcement Agency (NESREA) and the World Health Organization (WHO).

Adsorbent dosage and experimental conditions

A fixed dosage of 1.0 g per 50 mL of POME was used in all batch adsorption experiments. The adsorbent was prepared at different kaolinite clay-to-banana peel biochar (KC:BP) ratios to form a blend. 1:0 g, 0:1 g, 0.5:0.5 g, 0.75:0.25 g, and 0.25:0.75 g was prepared. The pH of the raw POME was measured prior to adsorption and recorded as 4.5 using a digital pH meter. All experiments were conducted at room temperature under controlled laboratory conditions and the obtained values were used for analysis.

Preparation of Standard Calibration Curve for Phosphorus

Standard phosphate solutions (0.0-3.0 mg/L) were prepared by diluting the stock phosphate solution with distilled water. To 10 mL of each standard solution, 8 mL of combined reagent was added and the mixture was allowed to stand for 10-12 minutes for colour development. Absorbance was measured at 600 nm using a UV-Vis spectrophotometer against a reagent blank. A calibration curve was obtained by plotting absorbance against phosphate concentration. The phosphorus concentration of the samples was determined by extrapolation from the calibration curve.

Preparation of bio-inorganic mixture (KC: BP)

Kaolinite clay was washed, dried using a Genlab drying oven (UK) at 110 °C, ground with a mortar and pestle and sieved through a 63-mesh sieve (0.241 mm) to obtain fine particles (Rosli et al., 2022). Banana peels were washed, dried, ground and pyrolyzed using a Carbolite CWF 1300 laboratory furnace (UK) at 325 °C for 30 min following the method of Selvarajoo et al. (2020), before sieving through a 63-mesh sieve. The bio-inorganic adsorbent was prepared by blending kaolinite clay and banana peel biochar in predetermined ratios of 1:0 g, 0:1 g, 0.5:0.5 g, 0.75:0.25 g, and 0.25:0.75 g (KC:BP), followed by adding water to obtain a homogeneous mixture. The resulting blends were oven-dried at 110 °C and stored in airtight containers for subsequent adsorption experiments.

Batch adsorption studies

Batch adsorption experiment was conducted to investigate the adsorption of phosphorus onto the blended bio-inorganic adsorbent. The adsorption parameters that was varied are the contact time, adsorbent ratio and agitation speed. All experiments were conducted at room temperature of 25 ^{0}C. 50 ml of the effluent was measured using a measuring cylinder and poured into a conical flask. Each of the blended adsorbents in different proportions were added to different effluents at constant volume. The conical flask was covered with foil to prevent spills during the experiment. The adsorption studies were then conducted under varying experimental conditions and each sample was placed in the water bath shaker (Zenrox PE-4310)**.** The phosphorus concentrations in the solution before and after adsorption were determined using a spectrophotometer **(**Spectronic 20).

Characterization of the bio-inorganic adsorbent

The characterization instruments used are Scanning Electron Microscope (SEM), Fourier Transform Infrared Spectroscopy (FTIR) and Energy Dispersive Spectroscopy (EDS). A Thermo Scientific Scanning Electron Microscope (USA) was used to examine the surface and morphology of the adsorbent particles. Fourier Transform Infrared Spectroscopy (Agilent Cary 630 FTIR Spectrometer, USA) was used to identify functional groups. Energy-dispersive microscopy (Thermo Scientific SEM, USA) was used to investigate the physical and chemical properties of the blended adsorbent.

Effect of contact time on phosphorus adsorption

The effect of contact time on the adsorption of phosphorus was carried out by agitating 50 ml of the effluent at an agitation speed of 175 rpm and an adsorbent ratio of 0.75:0.25 g in a conical flask. Contact time of 60, 75, 90, 105, 120 and 135 minutes were used. After agitation, the blended adsorbent was separated from the solution by filtering through Whatman filter paper into sample bottles. The concentration of phosphorus remaining in the solution after equilibration was determined. The percentage removal efficiency and the phosphorus adsorbed was calculated from equation 1 and 2 respectively.

$$\% \, Removal = \frac{C_o - C_f}{C_o} x100 \quad (1)$$

$$Q_t = \frac{(C_o - C_e)V}{D} \quad (2)$$

C_o is the initial concentration of phosphorus in wastewater (mg/L), C_f is the final concentration (mg/L), C_e is the equilibrium concentration (mg/L), V is volume (L), and D is the total adsorbent dosage (g)

Effect of adsorbent ratio on phosphorus adsorption

The effect of adsorbent ratio on the adsorption of phosphorus was carried out by agitating 50 ml of the effluent at an agitation speed of 175 rpm and a contact time of 90 minutes in a conical flask. The adsorbent in a mixing ratio of kaolinite clay and banana peel biochar (KC: BP) at 1:0, 0:1, 0.5:0.5, 0.75:0.25 and 0.25:0.75 g were used. After agitation, the blended adsorbent was separated from the solution by filtering through Whatman filter paper into sample bottles. The concentration of phosphorus remaining in the solution after equilibration was determined. Then, the percentage removal efficiency was calculated using Equation 1 and the amount of phosphorus adsorbed by the blended adsorbent was calculated using Equation 3.

$$Q_e = \frac{(C_o - C_e)V}{D} \quad (3)$$

Effect of agitation speed on phosphorus adsorption

The effect of agitation speed on the adsorption of phosphorus was carried out by agitating 50 ml of the effluent at an adsorbent ratio of 0.75:0.25 g and a contact time of 90 minutes in a conical flask. Agitation speeds of 100, 125, 150, 175, and 200 rpm were used. After agitation, the adsorbent was separated from the solution by filtering through Whatman filter paper into sample bottles. The concentration of phosphorus remaining in the solution after equilibration was determined. Then, the percentage removal efficiency was calculated from equation 1.

Adsorption isotherm model

Freundlich model

The Freundlich adsorption isotherm is commonly used to describe the equilibrium relationship between the amount of adsorbate adsorbed per unit mass of the adsorbent and the concentration of the adsorbate remaining in the solution (Sampranpiboon et al., 2014). This model is particularly useful for heterogeneous surfaces, as it assumes that adsorption occurs on sites with varying energies (Mohammad et al., 2021). Freundlich adsorption isotherm is expressed in equation 4 and 5 (Mohammad et al., 2021):

$$\mathrm{q_e} = \mathrm{K_f C^{1/n}} \quad (4)$$

$$\log \mathrm{q_e} = \log \mathrm{k_f} + \frac{1}{\mathrm{n}} \log \mathrm{C_e} \quad (5)$$

n is the constant related to the sorption efficiency and energy, K_f is the Freundlich constant indicating the adsorption capacity (L/g), q_e is the amount of adsorbate adsorbed per unit weight of the adsorbent (mg/g), C is the equilibrium concentration of the adsorbate in solution (mg/L)

The linearized form of the Freundlich isotherm is expressed in equation 5

Temkin model

The Temkin isotherm suggests that the heat of sorption decreases linearly with increasing surface coverage due to interactions between the adsorbent and adsorbate (Sampranpiboon *et al.,* 2014). The Temkin isotherm equation is formulated as in equation 6 and 7 (Edet & Ifelebuegu, 2020):

$$q_e = \frac{R_T}{b_T} \ln (k_t C_e) C \quad (6)$$

$$q_e = \frac{R_T}{b_T} \ln k_t + \frac{R_T}{b_T} \ln C_e \quad (7)$$

q_e is the amount of adsorbate adsorbed at equilibrium (mg/g), R_T is the universal gas constant (8.314 J/mol·K), b_T is the constant related to the heat of adsorption (J/mol), K_t is the equilibrium binding energy which corresponds to the optimum binding energy(dm^3/g), C_e is the equilibrium concentration (mg/L).

Temkin model can be represented linearly as shown in equation 7

Dubinin Radushkevich model

The D-R isotherm is important to determine the type of adsorption taking place i.e. physisorption or chemisorption. It also provides information on the mean adsorption energy. The D-R is calculated using equation 8 (Edet & Ifelebuegu, 2020):

$$\ln q_e = \ln QD - BD + (RT \ln \left(1 + \frac{1}{c_e}\right))^2 \quad (8)$$

QD is the maximum adsorption capacity (mol/g), BD is the D-R constant (mol²/kJ²), which can be determined from the slope and intercept of the linear plot of ln qe versus RT ln (1 + $\frac{1}{C_e}$)

Adsorption kinetic model

Pseudo first order

This model is commonly referred to as the Lagergren model and it helps to understand if the adsorption of the adsorbate with the adsorbent is a physisorption dominated process. The pseudo first order is calculated using equation 9 and 10 (Eletta *et al.,* 2016):

$$\frac{dq_t}{d_t} = k_t(q_e - q_t) \quad (9)$$

$$\ln q_e - q_t = lnq_e - k_1 \quad (10)$$

q_t is the amount of adsorbate adsorbed at time t (mg/g), q_e is the amount of adsorbate at equilibrium (mg/g), k_t is the rate constant for the pseudo-first-order model (min^{-1}).

The linear form of equation 9 can be obtained by integration and rearrangement as presented in equation 10

Pseudo second order

It helps to understand if the adsorption of the adsorbate with the adsorbent is a chemisorption dominated process (Eletta et al., 2016). The adsorption kinetics rate equation for the pseudo second order model is expressed in 11 and 12 (Eletta *et al.,* 2016):

$$\frac{dq_t}{d_t} = k_2(q_e - q_t)^2 \quad (11)$$

$$\frac{t}{q_t} = \frac{1}{k_2 q_e^2} + \frac{t}{q_e} \quad (12)$$

k_t is the rate constant for the pseudo-first-order model (min^{-1}), all other parameters have been defined.

The linear form of equation 11 can be obtained by integration and rearrangement as presented in equation 12

Intra particle diffusion

Intra particle diffusion model helps to determine whether the adsorption rate is controlled by intraparticle diffusion which is common for porous materials like biochar. The equations that was

adopted in the kinetic study are those adopted by Eletta *et al*., (2016) as shown in equation 13:

$$q = k_p t^{0.5} + C \quad (13)$$

q is the amount of solute adsorbed at time (mg/g), k_p is the intraparticle diffusion rate constant (mg/g.min), t is the contact time (min), C is the intercept (mg/g) which provides information about the thickness of the boundary layer.

Error function analysis

Error function analysis were employed to evaluate the accuracy and reliability of the isotherm model. The statistical error parameters used include the Sum of Squared Error (SSE), Average Relative Error (ARE %), Chi- square (X^2) and Root Mean Square Error (RMSE). These parameters provide a quantitative measure of deviation between the experimental and model predicted adsorption capacities. Lower values of these error functions indicate a better fit of the model to the experimental data.

Reusability study

The reusability of the blended bio-inorganic adsorbent was evaluated to assess its potential for sustainable phosphorus removal from POME (Al-sareji *et al.,* 2023). After each adsorption cycle, the mixture was separated from the treated POME by filtration, thoroughly washed with distilled water, and oven-dried in a Genlab drying oven (UK) at 105 °C until a constant weight was obtained. The regenerated adsorbent was reused under the same adsorption conditions for subsequent treatment cycles. This procedure was repeated for four consecutive cycles to evaluate the decline in adsorption performance and determine the effective reuse capacity of the adsorbent.

RESULTS AND DISCUSSION

Characterization of the blended bio-inorganic adsorbent

FTIR characterization before and after adsorption

The FTIR spectra of the blended bio-inorganic adsorbent before adsorption are presented in Fig 1(a-e). The broad adsorption bands observed around 3690-3694 cm^{-1} correspond to O-H stretching vibrations of hydroxyl groups in alcohols and phenolic compounds present in the blended adsorbent (Adesanmi et al., 2020; Alaa El-Dina et al., 2017). Peaks observed around 2881-2885 cm^{-1} are attributed to C-H stretching vibrations of aliphatic compounds. The adsorption bands within the range of 1000-1066 cm^{-1} are associated with C-O and Si-O stretching vibrations, indicating the presence of silicate minerals and oxygen-containing functional groups in the blended adsorbent.

After adsorption, noticeable changes in peak intensity and slight shifts in adsorption bands were observed in the FTIR spectra of the phosphorus-loaded blended adsorbent as shown in Fig 2. These changes suggest possible interactions between phosphate species and the functional groups present on the blended adsorbent's surface. The observed variations in hydroxyl and silicate-related bands may indicate their involvement in the adsorption process.

SEM characterization before and after adsorption

The SEM micrographs of the blended adsorbent before adsorption are shown in Fig 3(a–e). Fig 3a (0:1 g) exhibits a highly porous, rough surface with interconnected pores and irregular pathways, which may enhance adsorption by providing additional active sites (Adesanmi *et al.,* 2020). Fig 3b (1:0 g) shows irregularly shaped particles typical of kaolinite clay minerals (Rosli *et al.,* 2022). The bio-inorganic adsorbent exhibited varying surface morphologies as a function of the kaolinite-to-biochar ratio. Among the blended adsorbent, Fig 3d

(0.75:025 g) exhibited a relatively rough and porous surface structure which may contribute to improved adsorption performance. After adsorption, the SEM image in Fig. 4 revealed partial pore blockage and surface deposits on the blended adsorbent. These morphological changes may be associated with the attachment of phosphorus-containing species onto the adsorbent surface.

EDS characterization before and after adsorption

The elemental composition of the blended bio-inorganic adsorbent before adsorption is presented in Table 1. 0:1 g showed high carbon and oxygen contents, indicating the presence of organic constituents such as cellulose, lignin, and other carbonaceous materials (Adesanmi *et al.,* 2020). 1:0 g exhibited a high silicon content due to the silicate-based composition of kaolinite clay (Rosli *et al.,* 2022). The absence of phosphorus in the bio-inorganic adsorbent indicates that no phosphorus contamination was introduced by the adsorbent prior to treatment.

The EDS results after adsorption, presented in Table 2, revealed the presence of phosphorus on the adsorbent's surface at a weight concentration of 0.32%, suggesting phosphorus uptake from the POME. Changes in oxygen and potassium contents after adsorption may indicate the possible involvement of oxygen-containing functional groups and ion exchange during adsorption. Some minor elemental variations observed after adsorption could be attributed to the complex composition of POME or to instrumental and sample-preparation effects.

Batch adsorption experiment

Effect of Contact Time

The observed result as shown in Fig 5 indicated that the removal efficiency for the contact time 60, 75, 90, 105, 120 and 135 min are 70%, 80%, 88%, 90%, 91% and 92% respectively. The result showed that there is a gradual increase in the removal efficiency with increase in the contact time between 60 min - 90 min. Thereafter, there is a limited increase in contact time between 90 min - 135 min. The maximum removal efficiency of about 92% was observed at 135 min. This suggests that a 90 min contact time is optimal for removing phosphorus from the effluent.

Effect of adsorbent ratio

The results suggest that as the proportion of kaolinite clay in the blended adsorbent increases, phosphorus removal efficiency improves (Fig. 6). Similarly, phosphorus removal efficiency decreased as banana peel biochar increased. This suggests that kaolinite clay acts as a good adsorbent along with a minimum dosage of banana peel biochar. The efficiency of kaolinite clay in the removal of phosphorus can be attributed to the clay's high surface area, cation exchange capacity, and porous microstructure, which provides numerous active sites for adsorption, while the presence of banana peel powder in moderate proportion can contribute beneficial functional groups that enhance binding interaction (Adesanmi *et al.,* 2020; Rosli *et al.,* 2022; Ogundipe *et al.,* 2023). Therefore, 0.75:0.25 g can be considered as the optimum adsorbent ratio for the removal of phosphorus from the effluent.

Effect of agitation speed

The results suggest that the removal efficiency of phosphorus increases with increasing agitation speed as shown in Fig 7. The removal efficiency for agitation speeds of 100, 125, 150, 175 and 200 rpm are 64%, 73%, 80%, 87% and 90% respectively. The maximum removal efficiency occurs at 200 rpm. It can also be observed that removal efficiency increases gradually between 100 rpm and 175 rpm. At 175 rpm, there was a slight increment in the removal efficiency between 175 rpm and 200 rpm.

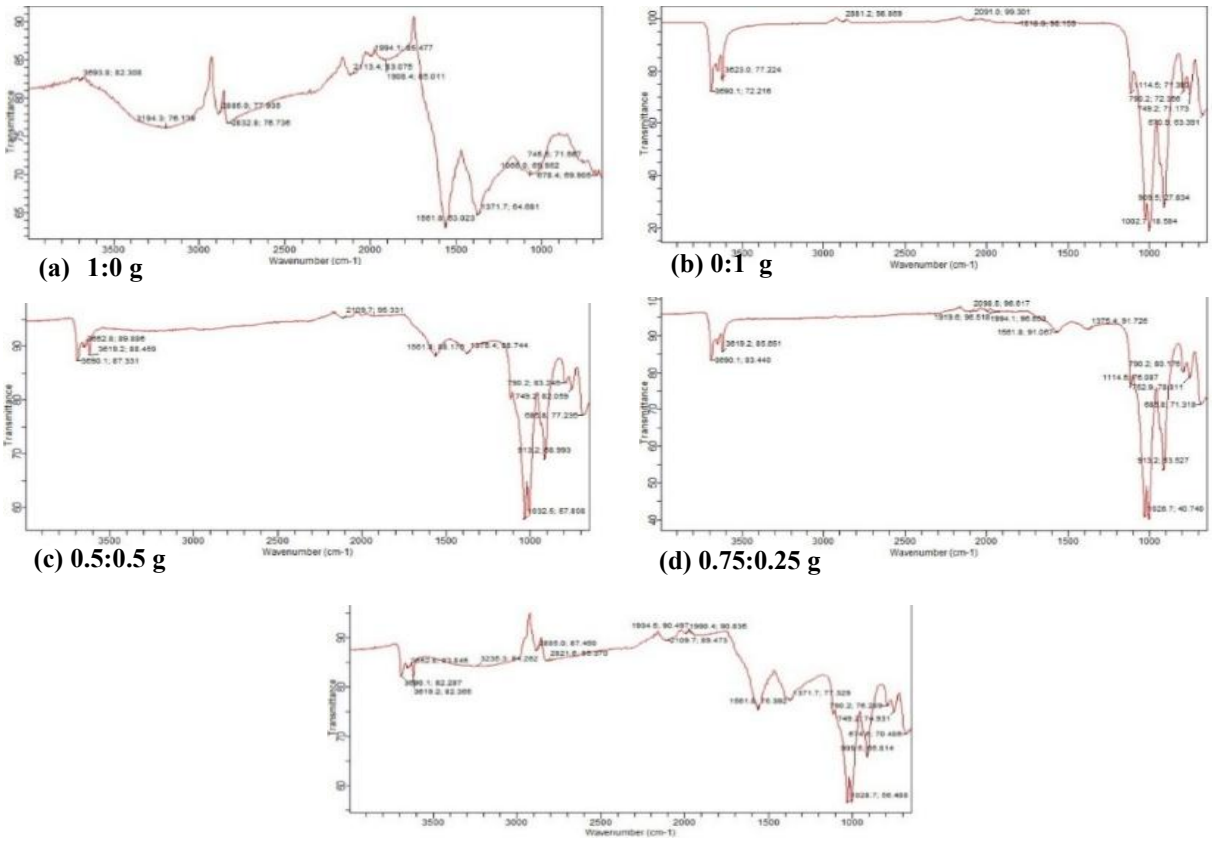

Figure 1: FTIR Analysis Spectra before adsorption

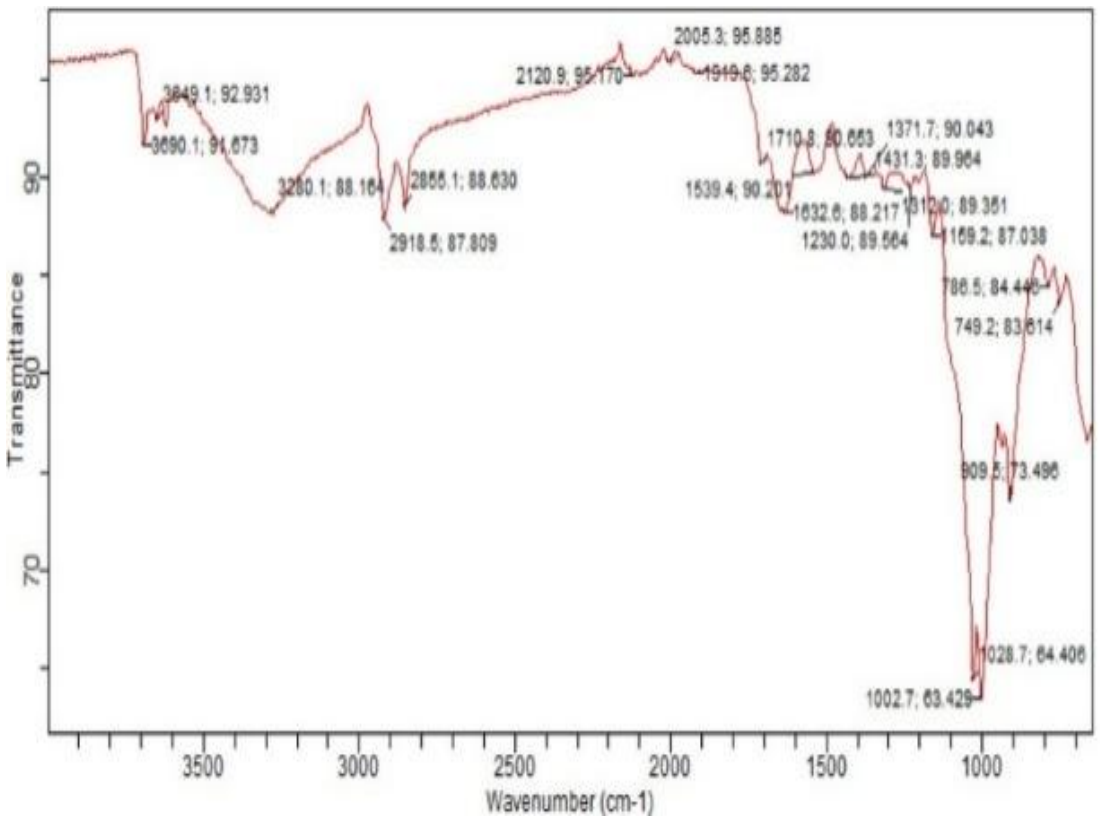

Figure 2: FTIR Analysis Spectra for 0.75:0.25 g after Adsorption

This suggests that 175 rpm is the optimal agitation speed for phosphorus removal efficiency from the effluent.

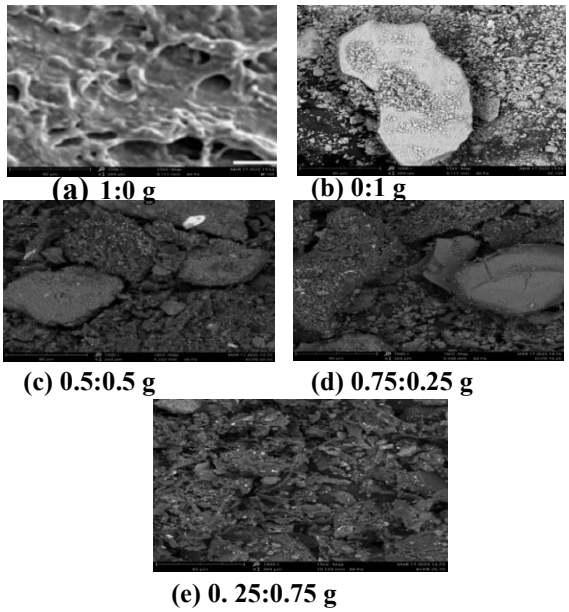

Figure 3: SEM Images before adsorption

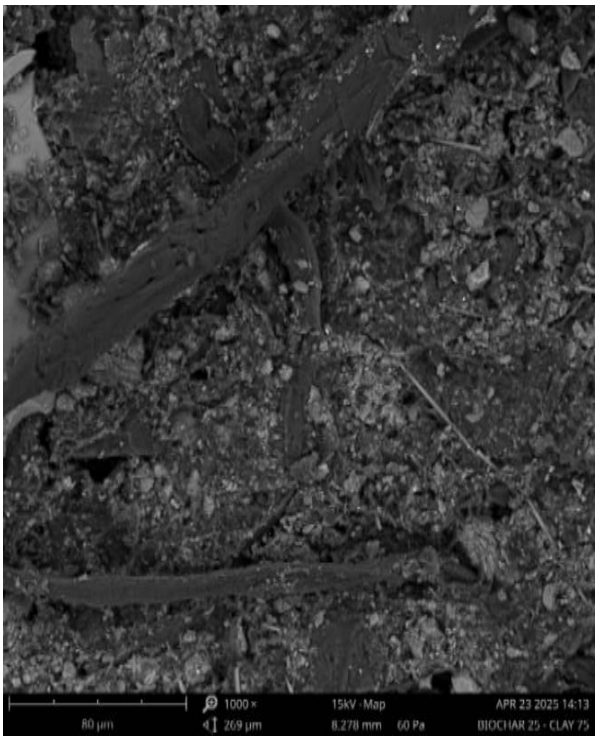

Figure 4: SEM Image for 0.75:0.25 g after Adsorption

Table 1: Elemental Composition of the Blended Bio-inorganic Adsorbent before Adsorption

Element Symbol	Element Name	Weight Concentration (%) KC: BP				
		1:0 g	0:1 g	0.5:0.5 g	0.75:0.25 g	0.25:0.75 g
Si	Silicon	0.20	63.75	8.12	12.71	3.82
Sr	Strontium	-	15.41	1.75	2.91	0.28
C	Carbon	50.70	14.64	41.34	35.71	53.27
Al	Aluminium	-	4.84	8.65	9.97	4.55
Zn	Zinc	-	0.68	-	-	0.37
Sn	Tin	-	0.52	0.78	1.42	3.24
Cl	Chlorine	-	0.17	0.58	0.36	1.04
Ca	Calcium	0.63	-	0.15	-	0.23
Na	Sodium	4.55	-	-	-	0.13
N	Nitrogen	3.20	-	2.92	3.48	1.17
K	Potassium	-	-	7.17	3.77	13.46
Ti	Titanium	-	-	0.76	0.21	-
O	Oxygen	35.23	-	27.74	29.23	18.02
P	Phosphorus	-	-	-	-	-
S	Sulfur	5.49	-	0.04	-	-

Adsorption isotherm model

The Freundlich model showed a good fit to the experimental data with a correlation coefficient of R^2 = 0.9733 as shown in Fig 8. The adsorption intensity (n= 1.33) indicated favorable adsorption of phosphorus onto the blended adsorbent surface, while the Freundlich constant (K_f= 0.184 L/g) suggested moderate adsorption capacity (Ikhazuangbe *et al.,* 2017; Kataya *et al.,* 2023). The results imply that adsorption may occur on a heterogeneous surface with possible multilayer formation. The Temkin model exhibited the best fit with a regression coefficient of R^2= 0.9957 as shown in Fig 9, indicating strong adsorbate-

adsorbent interactions. The Temkin constants (A= 0.620 L/g, b= 0.6175 mg/g) suggest that the heat of adsorption decreased gradually with increasing surface coverage, which is a characteristic of heterogeneous adsorption systems (Swelam et al., 2015; Jahin *et al.,* 2024). The D–R model showed a reasonable fit to the experimental data with R^2= 0.9422 as shown in Fig 10. The mean adsorption energy (E= 35.36 kJ/mol) suggests that chemisorption may be involved in the adsorption process since E > 16 KJ/mol (Mahanty *et al.,* 2023). This also suggests that the removal of phosphorus from POME by the blended adsorbent may involve a chemical bonding mechanism rather than weak physical forces.

Table 2: Elemental Composition of the Blended Bio-inorganic Adsorbent after Adsorption

Element Symbol	Element Name	Weight Concentration (%)
C	Carbon	47.44
Si	Silicon	18.03
O	Oxygen	10.95
Al	Aluminium	6.65
Sr	Strontium	3.97
N	Nitrogen	5.11
K	Potassium	1.77
Fe	Iron	1.76
Ca	Calcium	1.47
Ti	Titanium	1.17
Zr	Zirconium	0.61
S	Sulfur	0.46
P	Phosphorus	0.32
Cl	Chlorine	0.29

Adsorption kinetic model

The pseudo first order model showed a high correlation coefficient (R^2= 0.9895) indicating a good linear fit as shown in Fig 11. However, the calculated equilibrium adsorption capacity (Qe= 24.13 mg/g) differed significantly from the experimental value (2.38 mg/g), suggesting that the model may not adequately describe the adsorption kinetics of phosphorus onto the blended adsorbent.

The pseudo second order model showed a strong correlation coefficient (R^2 = 0.9788) as shown in Fig 12 with a calculated adsorption capacity (Qe = 3.397 mg/g) closer to the experimental value (2.380 mg/g). This suggests that the adsorption process may be better described by the pseudo second order model indicating possible involvement of chemisorption mechanisms (Liu *et al.,* 2023).

The intraparticle diffusion model indicated that pore diffusion was not the sole rate-limiting step as the plot did not pass through the origin and the intercept value was greater than zero as shown in Fig 13. This suggests that other mechanisms such as boundary layer diffusion and film diffusion may also contribute to the adsorption process (Liu *et al.,* 2023; Su *et al.,* 2021; Zhuang *et al.,* 2022).

Error function

Error function analysis was conducted to further evaluate the suitability of the adsorption isotherm models as shown in Fig 14. The Temkin isotherm exhibited the lowest values of Sum of Squared Error (SSE =0.003752), Average Relative Error (ARE = 2.8283%), Chi-square (X^2 = 0.005298) and Root Mean Square Error (RMSE = 0.02739), indicating the closest agreement between the experimental and predicted adsorption data. The Freundlich model showed moderate agreement while the Dubinin–Radushkevich model recorded the highest error values, suggesting a comparatively poorer fit. Overall, the error analysis further supports the suitability of the Temkin isotherm for describing phosphorus adsorption onto the blended adsorbent.

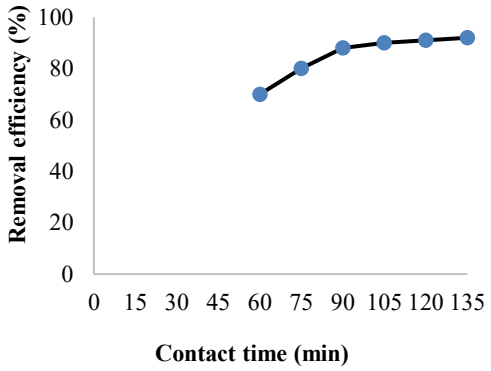

Figure 5: Effect of Contact Time on Phosphorus Removal Efficiency

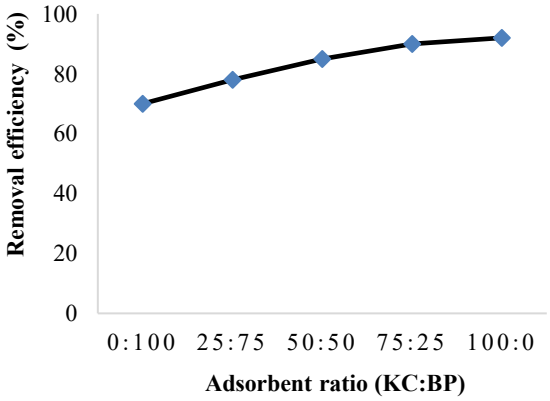

Figure 6: Effect of Adsorbent Ratio on phosphorus Removal Efficiency

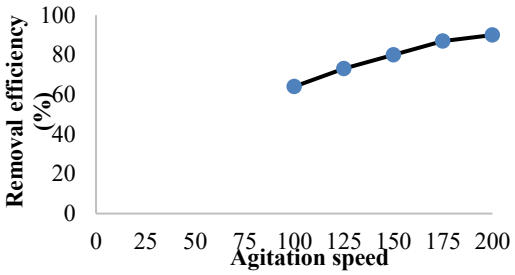

Figure 7: Effect of agitation speed on Phosphorus Removal Efficiency

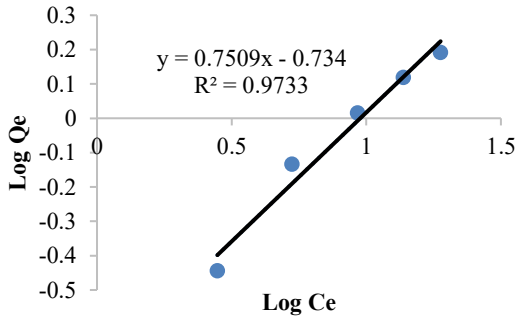

Figure 8: Freundlich isotherm plot for the adsorption of phosphorus

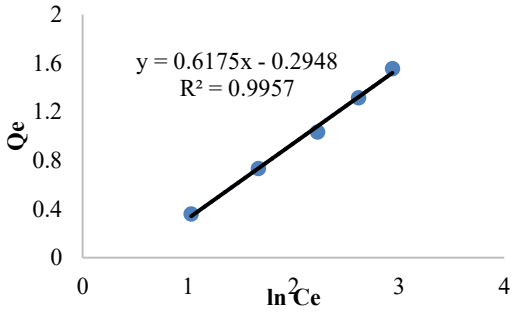

Figure 9: Temkin isotherm plot for the adsorption of phosphorus

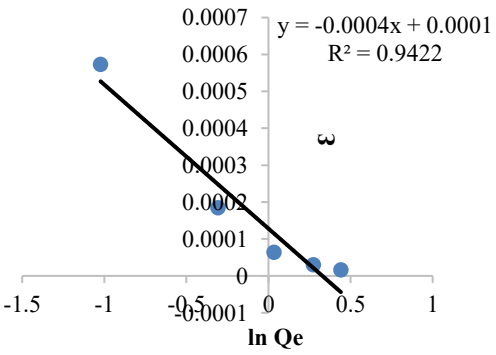

Figure 10: D-R isotherm plot for the adsorption of phosphorus

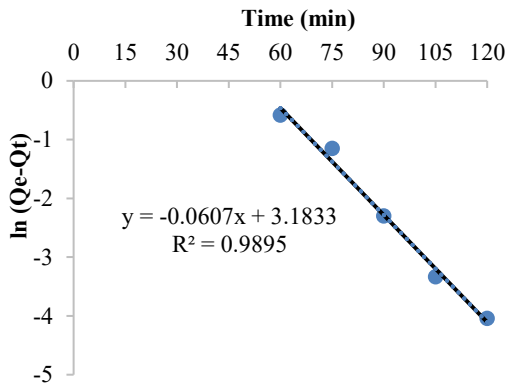

Figure 11: Pseudo first order plot for the adsorption of phosphorus

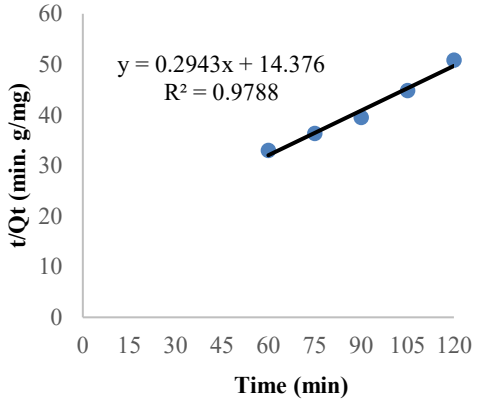

Figure 12: Pseudo second order plot for the adsorption of phosphorus

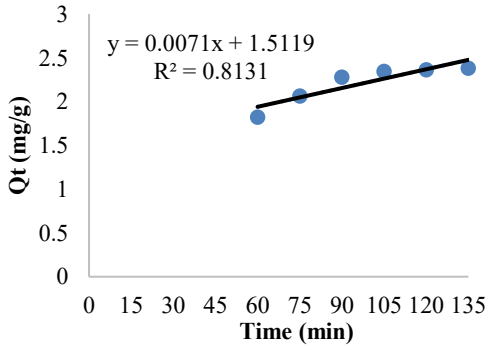

Figure 13: Intra-particle diffusion plot for the adsorption of phosphorus

Reusability study

The reusability study revealed a gradual decline in phosphorus removal efficiency with increasing reuse cycles as shown in Fig 15. The experiment was conducted under optimal conditions of a 0.75:0.25 g (KC:BP) adsorbent ratio, a 90 min contact time, and a 175 rpm agitation speed. During the first cycle, the blended adsorbent achieved 88% phosphorus removal, corresponding to a final concentration of 6.12 mg/L while the second cycle recorded 80% removal with a final concentration of 9.68 mg/L. A progressive decrease in adsorption performance was observed in subsequent cycles indicating a reduction in the availability of active adsorption sites. Although the blended adsorbent retained its adsorption capacity through the fifth cycle, a significant decline in removal efficiency was observed after the second cycle. This suggests that the blended adsorbent is reusable for phosphorus adsorption, but regeneration or replacement may be required after repeated use to maintain effective performance.

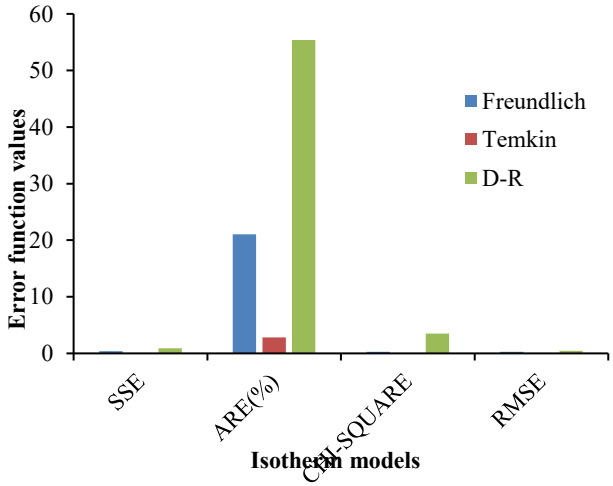

Figure 14: Error Function

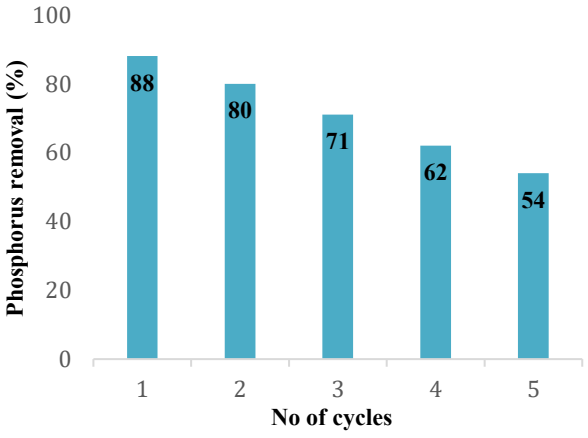

Figure 15: Reusability of the blended adsorbent

Table 3: Adsorption isotherm and kinetic constant values for phosphorus adsorption from POME

S/N	Pollutant removed	Adsorbent/ blended adsorbent	Equilibrium concentration/Removal efficiency	Reference
1.	Phosphorus	Kaolinite clay and Banana peel	6.12 mg/L 88%	This study
2.	Dyes and heavy metals	Banana Rachis and kaolinite clay	12.42 mg/L	Islam *et al.,* 2021
3.	Nitrate, phosphate and ammonium	Kaolinite clay	85%	Ogundipe *et al.,* 2023
4.	Nitrates	Banana peel and Orange peel	28 mg/L 86%	Kiran *et al.,* 2022
5.	Dye	Kaolinite clay	16.23 mg/L	Adebowale *et al.,* 2014

Table 4: Comparison of Adsorption Performance of Adsorbents with Reported Studies on Different Pollutants

Isotherm model	Variables	Phosphorus	Kinetic model	Parameters	Phosphorus
Freundlich	K_f (L/g)	0.184	Pseudo first order	$Q_{e(exp.)}$ (mg/g)	2.380
	n	1.33		$Q_{e(cal)}$ (mg/g)	24.130
	R^2	0.9733		k_1 (min^{-1})	0.0607
				R^2	0.9895
Temkin	A (L/g)	0.620	Pseudo second order	$Q_{e(exp.)}$ (mg/g)	2.380
	b (KJ/mol)	4.01		$Q_{e(cal)}$ (mg/g)	3.397
	B	0.6175		k_1 (min^{-1})	0.00602
	R^2	0.9957		R^2	0.9788
Dubinin Radushkevich	Qmax (mg/g)	1.0001	Intra-particle diffusion	$Q_{e(exp.)}$ (mg/g)	2.380
	B	0.0004		$Q_{e(cal)}$ (mg/g)	-
	E (KJ/mol)	35.36		k_1 (min^{-1})	0.0071
	R^2	0.9422		R^2	0.8131

CONCLUSION

This study demonstrated the potential of a kaolinite-banana peel biochar blended adsorbent for phosphorus removal from palm oil mill effluent (POME). The blended adsorbent achieved optimum phosphorus removal efficiency of 88% under the operating conditions of 0.75:0.25 g (KC:BP) adsorbent ratio, 90 min contact time and 175 rpm agitation speed, reducing the phosphorus concentration from 51.72 mg/L to 6.12 mg/L. The adsorption capacity under these conditions was 2.38 mg/g. FTIR, SEM and EDS analysis further explained the interaction of phosphorus species with the blended adsorbent. Adsorption kinetics were better described by the pseudo second order model while the Temkin isotherm provided the best fit for the equilibrium data, suggesting possible chemisorption and adsorbate–adsorbent interactions. The reusability study showed that although the blended adsorbent retained adsorption capability over multiple cycles, a gradual decline in removal efficiency was observed with repeated use.

The kaolinite-banana peel biochar blended adsorbent shows promising potential as a low-cost and sustainable adsorbent for phosphorus removal from complex wastewater systems such as POME.

Data availability

The datasets used and/or analyzed in this study are accessible in the publication and can be obtained upon request from the corresponding author.

Competing interest

The authors declare that there is no conflict of interest.

Funding

The authors received no specific funding for this work

Author Contribution

The authors performed all research activities including conceptualization, methodology, investigation, data analysis, and manuscript preparation.

REFERENCES

Adams, F. D., Joseph, M. V, & Shettima, B. (2017). Geochemical investigation of clay minerals in Marte, Borno state, Nigeria. *Arid Zone Journal of Engineering, Technology and Environment (AZOJETE)*, *13*(5), 544–554.

Abdoli, S., Asgari Lajayer, B., Dehghanian, Z., Bagheri, N., Vafaei, A. H., Chamani, M., & Price, G. W. (2021). A Review of the Efficiency of Phosphorus Removal and Recovery from Wastewater by Physicochemical and Biological Processes: Challenges and Opportunities. Water, 16(17), 2507.

Adebowale, K. O., Olu-Owolabi, B. I., & Chigbundu, E. C. (2014). Removal of safranin-O from aqueous solution by adsorption onto kaolinite clay. Journal of Encapsulation and Adsorption Sciences, 4(3), 89.

Adesanmi, A. S., Evuti, A. M., Aladeitan, Y. M., & Abba, A. H. (2020). Utilization of waste in solving environmental problem: application of banana and orange peels for the removal of lead (ii)ions from aqueous solution of lead nitrate. Nigeria Journal of Engineering Science and Technology Research, 6(1), 18-33.

Alaa El-Dina, G., Amerb, A., Malsha, G., & Hussein, M. (2017). Study on the use of banana peels for oil spill removal. Alexandria Engineering Journal, 57(3), 2061 – 2068.

Al-Ghouti, M. A., & Da'ana, D. A. (2020). Guidelines for the use and interpretation of adsorption isotherm model: A review. Journal of hazardous materials, 393.

Ali, I., Asim, M., & Khan, T. (2019). Low cost adsorbents for the removal of organic pollutants from wastewater. Journal of environmental management, 113, 170-183.

Al-sareji, O., Abdulzahra, M., Hussein, T., Shlakaa, A., Karhib, M., & Meiczinger, M. (2023). Removal of pharmaceuticals from water using laccase. Water, 15(19), 3437.

Al-Swadi, H. A., Al-Farraj, A. S., Al-Wabel, M. I., Ahmad, M., Ahmad, J., Mousa, M. A., & Usama, M. (2023). Kaolinite-composited biochar and hydrochar as low-cost adsorbents for the removal of cadmium, copper, lead, and zinc from aqueous solutions. Sustainability, 15, 15978.

Edet, U. A., & Ifelebuegu, A. O. (2020). Kinetics, isotherms, and thermodynamic modeling of the adsorption of phosphates from model wastewater using recycled brick waste. Processes, 8(6), 665.

Eletta, O., Ajayi, O., Ogunleye, O., & Akpan, I. (2016). Adsorption of cyanide from aqueous solution using calcinated eggshells: Equilibrium and optimisation studies. Journal of Environmental Chemical Engineering, 4(1), 1367-1375.

Ikhazuangbe, P. M., Kamen, F. L., Opebiyi, S. O., Nwakaudu, M. S., & Onyelucheya, O. E. (2017). Equilibrium isotherm, kinetic and thermodynamic studies of the adsorption of erythrosine dye onto activated carbon from coconut fibre. International Journal, 4(5), 2356-1908.

Islam, M. M., Islam, M. S., Maniruzzaman, M., Haque, M. M., & Mohana, A. A. (2021). Banana rachis CNC/Clay composite filter for dye and heavy metals adsorption from industrial

wastewater. Engineering Science & Technology, 2(1), 140-152.

Jahin, H., Khedr, A., & Ghannam, H. E. (2024). Banana peels as a green bioadsorbent for removing metals ions from wastewater. Discover Water, 4(1), 36.

Kasmuri, N., Kasim, Z., Aziz, A. A., & Ismail, N. A. (2023). Factorial Design for Optimization and Performance Evaluation of Palm Oil Mill Effluent (POME) using Electrocoagulation. Biointerfacr Research in Aplied Chemistry, 13(6), 564.

Kataya, G., Issa, M., Jeguirim, M., & Hijazi, A. (2023). Characterization and Environmental Application Potential of Banana Peels Biochar. Engineering Proceedings, 37(1), 105.

Kiran, P. V., Ramu, M. N., Nagendra, V. S., & Krishna, J. S. (2022). Removal of nitrates from water by environmental waste materials. International Journal of Engineering Research and Application, 12(1) 48-52.

Liu, R., Li, Y., Zhao, Z., Liu, D., Ren, J., & Luo, Y. (2023). Synthesis and characterization of clay-biochars produced with facile low-temperature one-step in the presence of air for adsorbing methylene blue from aqueous solution. Frontiers in Envronment Science, 11, 1137284.

Mahanty, B., Behera, S., & Sahoo, N. (2023). Misinterpretation of Dubinin–Radushkevich isotherm and its implications on adsorption parameter estimates. Separation Science and Technology, 58(7), 1275-1282.

Mohammad, S., Baidurah, S., Kobayashi, T., Ismail, N., & Leh, C. (2021). Palm oil mill effluent treatment processes- A review. Processes, 9, 739. Retrieved from https://doi.org/10.3390/pr9050739.

Narayana Saibaba, K. (2022). Kaolinite-Chitosan based Nano-Composites and Applications. Advanced Applications of Micro and Nano Clay: Biopolymer-based Composites, 125.

Norhafezah, K., Zulhelmi, K., Aina, A., Nor, A., & Muhammad, S. (2023). Factorial Design for Optimization and Performance Evaluation of Palm Oil Mill Effluent (POME) using Electrocoagulation. Open-Access Journal, 13(6), 564.

Ogundipe, F. O., Saidu, M., Abdulkareem, A. S., & Busari, A. O. (2023). Isotherm and Thermodynamic Adsorption Studies of Nitrate, Phosphate and Ammonium on to Beneficiated Kaolin Clay from Kutigi, Niger State, Nigeria. Journal of Inventive Engineering and Technology, 3(1), 89-98.

Okereke, J. N., & Ginikanwa, R. C. (2020). Environmental impact of palm oil mill effluent and its management through biotechnological approaches. International Journal of Advanced Research in Biological Science, 7(7), 112-127.

Rosli, M. H., Siyal, A. A., Shamsuddin, R. M., & Low, A. (2022). Feasibilty of kaolin and mica as bleaching earths for the removal of organic compounds from crude palm oil. Jurnal Teknologi, 85(5), 145-154.

Sampranpiboon, P., Charnkeitkong, P., & Feng, X. (2014). Equilibrium isotherm models for adsorption of zinc (II) ion from aqueous solution on pulp waste. WSEAS Transactions on Environment and Development, 10, 35-47.

Selvarajoo, A., Muhammad, D., & Arumugasamy, S. K. (2019). An experimental and modelling approach to produce biochar from banana peels through pyrolysis as potential renewable energy resources. Modeling Earth Systems and Environment.

Singh, S., Sharma, A., & Malviya, R. (2021). Industrial wastewater: health concern and treatment strategies. The Open Biology Journal, 9(1).

Song, J., Zhang, S., Li, G., Du, Q., & Yang, F. (2020). Preparation of montmorillonite modified biochar with various temperatures and their mechanism for Zn ion removal. J. Hazard. Mater., 391. doi:121692

Su, L., Zhang, H., Oh, K., Liu, N., Luo, Y., Cheng, H., & He, X. (2021). Activated biochar derived from spent Auricularia auricula substrate for the efficient adsorption of cationic azo dyes from single and binary adsorptive system. Water Science and Technology, 84(1), 101-121.

Swelam, A., El-Nawawy, M., Awad, M., & El-Mahallawy, M. S. (2015). Selective Removal for Toxic Ions from Aqueous Environment Using Ion Exchange Resin. International Journal of Environment, 4(1), 1-12.

Utibe, A., Uduak, U., Opeyemi, K., Otobong, D., Solomon, E., Nnanake-Abasi, O., & Nnamso, D. J. (2024). Emerging trends in POME treatment and applications: chemical and biotechnological aspects. Journal of Materials & Environmental Sustainability Research, 4(1), 11-44.

Zahed, M. A., Salehi, S., Tabari, Y., Farraji, H., Ataei-Kachooei, S., Zinatizadeh, A. A., & Mahjouri, M. (2022). Phosphorus removal and recovery: state of the science and challenges. Environmental Science and Pollution Research, 25(39), 58561–58589.

Zhuang, J., & Yu, G. R. (2022). Effects of surface coatings on electrochemical properties and contaminant sorption of clay minerals. Chemosphere, 49(6), 619-628.